Numerical Simulation of the Wind-Stress Effect on SAR Imagery of Far Wakes of Ships

Atsushi Fujimura, Alexander Soloviev, and Vladimir Kudryavtsev

***Abstract*—Centerline wakes of ships in synthetic aperture radar (SAR) images were modeled in 2-D with the computational fluid dynamics (CFD) software Fluent and a radar-imaging algorithm. We initialized the model with a pair of vortices generated by a ship hull and applied wind stress perpendicular to the ship wake. Results of the CFD simulation using a nonhydrostatic model have demonstrated ship-wake asymmetry with respect to the wind-stress direction relative to the ship course. Due to the wind stress, flow convergence increased on the upwind side of the centerline wake and reduced on the downwind side of the wake. The radar-imaging algorithm processed with the surface velocity field produced by the CFD model revealed ship-wake asymmetry relative to the wind direction. These results are qualitatively consistent with SAR images from the TerraSAR-X satellite and representative statistics of photographic images of the ship wake collected from a volunteer observing ship.**

***Index Terms*—Hydrodynamics, numerical analysis, remote sensing, sea surface, synthetic aperture radar (SAR).**

I. Introduction

CENTERLINE wakes of surface ships can persist for a relatively long time and extend to tens of kilometers in synthetic aperture radar (SAR) images [1]. Studies of ship-wake hydrodynamics and remote sensing are important for ship detection, oceanic safety, and fishing and pollution control.

A wake beyond ten lengths of a ship is defined in this letter as the far wake of the ship. Hydrodynamics of far wakes of ships and environmental conditions of their visibility on SAR images have not yet been well understood. In this letter, we have numerically simulated and reproduced the effect of wind stress in SAR imagery of far wakes of ships—the asymmetry of the ship wake with respect to the wind direction. This effect had been noticed in the images of the National Aeronautics and Space Administration Seasat satellite [2] and was later found in photograph [3] and TerraSAR-X [4] images of ship wakes.

We have used the computational fluid dynamics program Fluent and a real aperture-radar-imaging algorithm for conceptual simulations of SAR images of the far wakes of ships under different environmental conditions. In this letter, we analyze the effect of wind stress on ship-wake dynamics and radar images.

This letter's content is as follows. Section II describes the numerical model that has been used for the simulation of ship-wake hydrodynamics. This section also contains a description of the radar-imaging algorithm as well as the available remote sensing and field data. Section III presents the main results of this letter. Section IV is devoted to discussion of the results and conclusions.

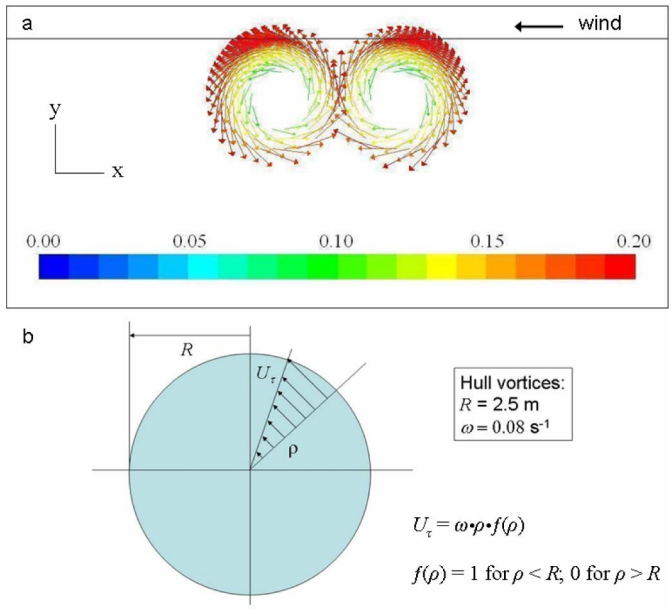

Fig. 1. (a) Initial velocity vectors of counterrotating vortex pair colored by velocity magnitude (meters per second); (b) radial structure of the vortex.

II. Model and Methods

A. Numerical Model

A 2-D mesh (horizontal length of 100 m × 30-m depth) was generated by the software package Gambit. The computational domain was sufficiently large in order to reduce the effects of boundaries. There were 240 000 rectangular cells. The cell size in the horizontal direction ($\Delta x = 2.5 \cdot 10^{-2}$ m) was made homogeneous. In the vertical direction, the cell size was increasing with a 1.1 growth rate from $\Delta y = 1.0 \cdot 10^{-2}$ m at the top of the domain to approximately $\Delta y = 2.5$ m near the bottom of the domain. The mesh required fine resolution at the top of the domain in order to resolve the wind-drift current in the near-surface layer of water.

A pair of counterrotating vortices, which mimicked a vortex pair created by a ship hull, was used as an initial condition (Fig. 1). Each vortex was 2.5 m in radius, and its angular velocity was 0.08 rad $\cdot$ s^{-1}. We were not trying to model the wake of any specific ship, but based on the study by Reed *et al.* [5],

Manuscript received July 28, 2009; revised December 10, 2009.

A. Fujimura and A. Soloviev are with the Nova Southeastern University Oceanographic Center, Dania Beach, FL 33004 USA (e-mail: fujimura@nova.edu; soloviev@nova.edu).

V. Kudryavtsev is with the Nansen Environmental and Remote Sensing Center, 5006 Bergen, Norway, and also with the Nansen International Environmental and Remote Sensing Center, 197101 St. Petersburg, Russia (e-mail: kvn@niersc.spb.ru).

Digital Object Identifier 10.1109/LGRS.2010.2043920

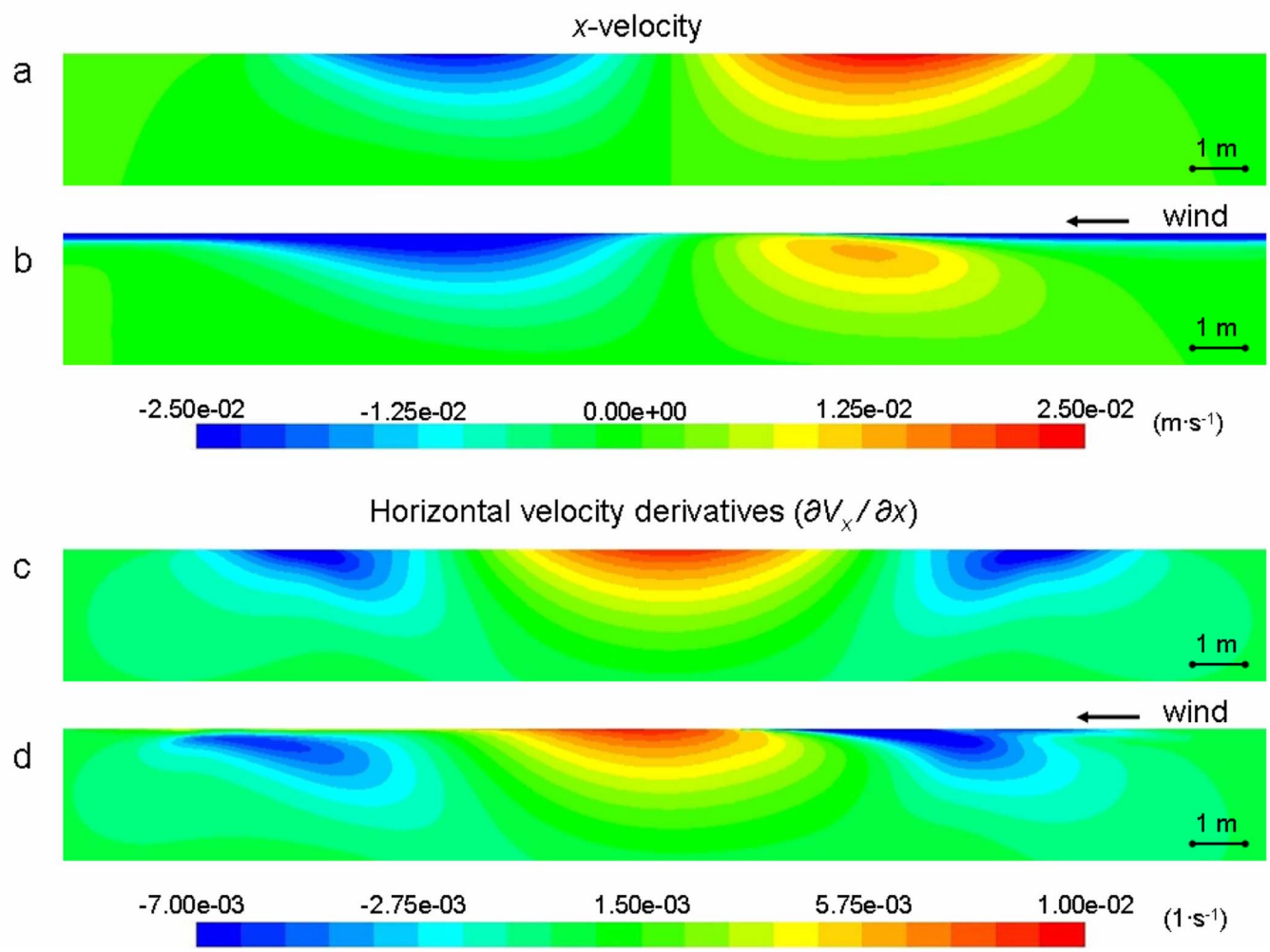

Fig. 2. Color contours on 2-D vertical planes focused on top layer after 200 s (8000 time steps): (a) and (b) Horizontal (x) velocity. (c) and (d) Horizontal-velocity derivatives $(\partial V_x/\partial x)$. (a) and (c) No wind stress. (b) and (d) Wind stress of 0.1 N $\cdot$ m^{-2} applied from right to left and corresponding to approximately 8.5 m $\cdot$ s^{-1} at a 10-m height. For the horizontal-velocity derivatives, blue indicates convergence zones, and red indicates divergence zones.

the vortices with these parameters could be observed at 64-m distance aft the stern of a ship with 75-m length, 10-m beam, and a forward speed of 10 kn.

The boundary condition at the top of the domain was a slip wall, and the sides of the domain were periodic in order to apply the wind-stress laterally. The wind stress was applied to the top boundary as a shear stress $\tau = 0.1$ N $\cdot$ m^{-2}, which was equivalent to approximately 8.5 m $\cdot$ s^{-1} wind at a 10-m height in open-ocean conditions.

A standard k–ω viscous model was used with the default Fluent parameters. The standard k–ω is an empirical model based on model transport equations for the turbulence kinetic energy (k) and the specific dissipation rate (ω), which can also be thought of as a ratio of dissipation rate to k [6]. The model was run with a constant time step $\Delta t = 0.025$ s. We spun up the model without the vortex pair and wind stress from 0 to 100 s, and then added the vortex pair or the vortex pair and wind stress at time 100 s to it and ran from 100 to 200 s. For further analysis, we used a segment from 175 to 200 s. In an additional run, we spun up the model without the vortex pair but with wind stress for the first 100 s and then added the vortex pair; however, no qualitative difference in the model results was observed for the time period from 175 to 200 s relative to the previous case.

B. Grid-Convergence Test

For model validation purposes, six grid-convergence tests were performed using different cell sizes. We have tested five combinations of homogenous horizontal cell sizes from $\Delta x = 2.5 \cdot 10^{-2}$ m down to $\Delta x = 0.5 \cdot 10^{-2}$ m and of vertical sizes at the surface from $\Delta y = 2.5 \cdot 10^{-2}$ m down to $\Delta y = 0.5 \cdot 10^{-2}$ m with 1.1 growth rate with depth.

C. Radar-Imaging Algorithm

Horizontal velocities (along the x-coordinate) on the surface were obtained every 0.5 s from the simulation in Fluent to produce a time-dependent velocity field. The velocity field from the top layer was used as an input into the real aperture-radar simulation algorithm developed by Kudryavtsev *et al.* [7]. The radar-imaging algorithm simulates both wind waves (in the range from spectral peak-wind waves to capillary waves) and radar backscattering at arbitrary geometry of radar observation. The calculation was performed for X-band, HH polarization,

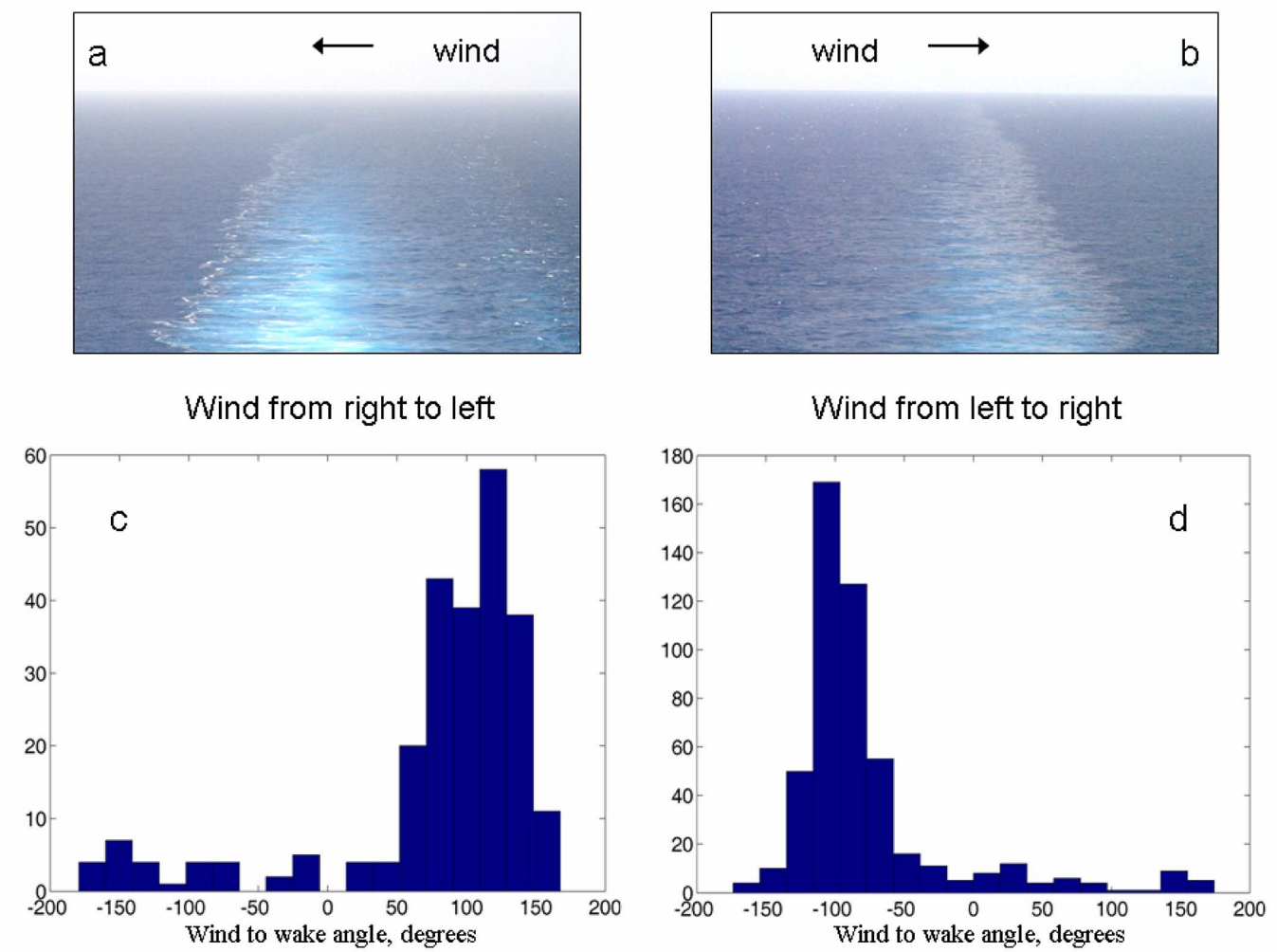

Fig. 3. (a) and (b) Examples of photographic images of the ship-wake asymmetry due to wind-stress effect. (c) and (d) Wake asymmetry statistics. Vertical axis represents the number of photograph images where only the (c) starboard- or (d) port-side wake boundary is sharp. Horizontal axis is wind direction relative to wake direction in degrees. Winds are more than 5 $m \cdot s^{-1}$. Wind direction is defined according to the meteorological convention; wake direction is defined as opposite to ship course. Positive values of wind to wake angle correspond to the wind from the port side [10].

and incidence angle of 30°. Due to relatively small velocity magnitudes associated with the water circulation in far wakes of ships (less than 0.1 $m \cdot s^{-1}$), the Doppler effect (intrinsic to SAR algorithms) should not lead to a significant difference between real and SAR images [8], [9].

D. Field Data

During a yearlong experiment on a volunteer observer ship, the Royal Caribbean Explorer of the Seas, Soloviev *et al.* [3] obtained a large amount of photographic images of the ship wake. The Atmospheric and Oceanic Laboratory, operated on this ship by the University of Miami Rosenstiel School of Marine and Atmospheric Science, has provided detailed information about the environmental conditions and ship telemetry during this experiment. Those images were statistically sorted by degrees of wind directions relative to wake directions [10].

III. Results

An example of the horizontal velocity and horizontal-velocity gradient fields produced by the model is shown in Fig. 2. Without wind stress [Fig. 2(a) and (c)], the circulation in the wake is symmetric. When the wind stress is applied, both horizontal velocity and its derivative (representing the surface-flow divergence) are skewed [Fig. 2(b) and (d)]. Furthermore, the downwind convergence zone appeared to be detached from the surface [Fig. 2(d)]. In other words, the downwind side of the wake is more diverged, and the upwind side of the wake is more converged than in the wake without wind stress. Model runs with larger wind stress (12 $m \cdot s^{-1}$) revealed the same pattern.

This ship-wake asymmetry with respect to the wind direction can be seen in photograph images taken from the Explorer of the Seas (Fig. 3). Results of the statistics in Fig. 3 show a strong correlation of the wind direction relative to ship course and the visibility of sharp-wake boundaries. The downwind side of the ship wake appears to be better resolved in the photograph images.

High-resolution SAR images from Seasat [2] and more recently from TerraSAR-X [an example is given in Fig. 4(a)] reveal the asymmetry of ship wakes with respect to wind direction. The result of the radar-imaging model [Fig. 4(b)], which has been run with the simulated sea-surface velocity

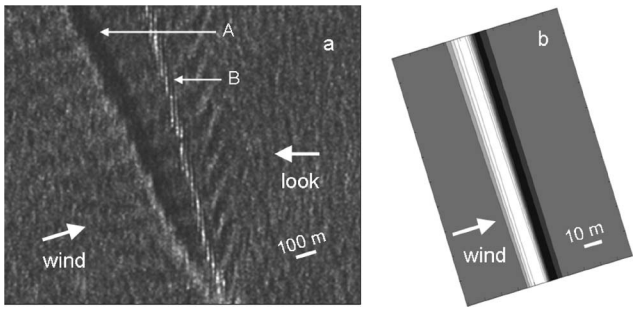

Fig. 4. (a) TerraSAR-X satellite image of a ship wake in the Strait of Gibraltar. Directions of wind and radar look are shown. The wind direction is tentative. (A) turbulent centerline wake. (B) Kelvin arm. (Credit: German Airspace Center (DLR); date: July 9, 2007, 06:29 UTC; original resolution: 3 m (reduced image); mode: StripMap mode; polarization: HH; incidence angle: 31.681°–34.688°; available from the DLR Web Site http://www.dlr.de/en/DesktopDefault.aspx/tabid-4313/6950_read-10126/gallery-1/gallery_read-Image.1.3759/). (b) Simulated radar image. Scale is only for horizontal direction (width of the wake). Time period is from 175 to 200 s.

field as an input, also shows ship-wake asymmetry. The wind stress is applied perpendicular to the centerline wake, and the asymmetry is consistent with the TerraSAR-X image of a ship wake shown in Fig. 4(a). The upwind side of the centerline wake is bright, and the downwind side of the wake is dark, both in the SAR image [Fig. 4(a)] and in the output of the radar-imaging algorithm [Fig. 4(b)]. The dark side is a divergence zone, where sea-surface roughness is suppressed and the radar signature is increased. In contrast, the sea-surface roughness and radar scattering are enhanced in the convergence zone on the upwind sides of the centerline wake, which is brighter.

Note that only one of the two Kelvin arms (Kelvin wake) is visible in Fig. 4(a). This might be due to the fact that the signatures of Kelvin arms are strongest when the direction of the crests of the cusp waves is normal to the radar look direction, and weakest when it is parallel to the look direction. Wind and other factors might also contribute to the radar signature of Kelvin arms as discussed by Hennings *et al.* [11]. The Kelvin wake is, however, beyond the scope of this letter.

IV. Discussion and Conclusion

The model results were qualitatively consistent with available SAR and photographic images. The ship-wake asymmetry in SAR due to wind–wake interaction can be reproduced qualitatively with the nonhydrostatic model (Fluent) and the radar-imaging algorithm. Wind stress enhances surface-flow convergence on the upwind side of the ship wake while suppressing it on the downwind side of the wake.

Grid-convergence tests (Section II-B) showed that simulation results of all the mesh sizes have qualitatively the same feature of ship-wake asymmetry. Spatial discretization error should asymptotically approach zero; however, it is difficult to have an ideal grid size because of computational cost. It would be compromised with a grid size which can achieve quantitatively validated results.

In this letter, we have used the standard k–ω turbulence closure scheme. For a quantitative-level simulation, the adjustable constants in the turbulence parameterization may need fine tuning, and the model results need to be validated with field data. Free surface, waves, temperature, surfactants, bubbles, and other possible factors might be important, and they also need to be included.

For more realistic modeling, 3-D simulations with vortices of the ship's screws are necessary because longitudinal velocities (along the wake) should be taken into account. The 3-D domain for a ship wake is much larger than that of a 2-D domain, and the fine-mesh resolution applied in 2-D is not feasible in 3-D, so mesh design should be optimized to accomplish the best results. Simulations for the 3-D model with velocities of screws are in progress [12].

Acknowledgment

The authors would like to thank M. Gilman [Nova Southeastern University Oceanographic Center (NSUOC)] for providing significant help in the implementation of the numerical simulation in Fluent and development of the mesh validation scheme; S. Matt [NSUOC and University of Miami Rosenstiel School of Marine and Atmospheric Science (UM RSMAS)] for useful discussion; J. Fenton (NSUOC) for technical help in finalizing the manuscript; E. Williams, C. Maxwell, and Don Cucchiara (UM RSMAS) for their help in conducting the experiment on the Explorer of the Seas; and the UM RSMAS and the Royal Caribbean International for accommodating our experiment on the Explorer of the Seas. This work is a part of the project "Hydrodynamics and remote sensing of far wakes of ships" at NSUOC.

References

[1] A. M. Reed and J. H. Milgram, "Ship wakes and their radar images," *Annu. Rev. Fluid Mech.*, vol. 34, pp. 469–502, Jan. 2002.
[2] T. Wahl, K. Eldhuset, and Å. Skelv, "Ship traffic monitoring using the ERS-1 SAR," in *Proc. 1st ERS-1 Symp.*, Cannes, France, 1992, pp. 823–828.
[3] A. Soloviev, M. Gilman, K. Moore, K. Young, and H. Graber, "Hydrodynamics and remote sensing of far wakes of ships," in *Proc. SEASAR Workshop*, Frascati, Italy, 2008.
[4] A. Soloviev, M. Gilman, K. Young, S. Brusch, and S. Lehner, "Sonar measurements in ship wakes simultaneous with TerraSAR-X overpasses," *IEEE Trans. Geosci. Remote Sens.*, vol. 48, no. 2, pp. 841–851, Feb. 2010.
[5] A. M. Reed, R. F. Beck, O. M. Griffin, and R. D. Peltzer, "Hydrodynamics of remotely sensed surface ship wakes," *SNAME Trans.*, vol. 98, pp. 319–363, 1990.
[6] *Fluent User's Guide*, Fluent Inc., Lebanon, NH, 2006.
[7] V. Kudryavtsev, D. Akimov, J. Johannessen, and B. Chapron, "On radar imaging of current features: 1. Model and comparison with observations," *J. Geophys. Res.*, vol. 110, no. C7, p. C07 016, Jul. 2005.
[8] I. G. Cumming and F. H. Wong, *Digital Processing of Synthetic Aperture Radar Data: Algorithms and Implementation*. Boston, MA: Artech House, 2005.
[9] K. Eldhuset, "An automatic ship and ship wake detection system for spaceborne SAR images in coastal regions," *IEEE Trans. Geosci. Remote Sens.*, vol. 34, no. 4, pp. 1010–1019, Jul. 1996.
[10] M. Gilman, K. Moore, K. Young, and A. Soloviev, "Photographic study of far wake of the Explorer of the Seas," Nova Southeastern Univ. Oceanographic Center, Dania Beach, FL, Tech. Rep. 002, Aug. 2008.
[11] I. Hennings, R. Romeiser, W. Alpers, and A. Viola, "Radar imaging of Kelvin arms of ship wakes," *Int. J. Remote Sens.*, vol. 20, no. 13, pp. 2519–2543, Sep. 1999.
[12] A. Fujimura and A. Soloviev, "Approaches to validation of CFD models for far ship wake," *Eos Trans. AGU*, vol. 89, no. 53, 2008, Fall Meet. Suppl., Abstract OS51B-1260.